Carbohydrate Research 344 (2009) 1863–1871

Contents lists available at ScienceDirect

Carbohydrate Research

journal homepage: www.elsevier.com/locate/carres

Microrheological investigations give insights into the microstructure and functionality of pectin gels

Romaric R. Vincent, Martin A. K. Williams *

Institute of Fundamental Sciences, Massey University, Palmerston North, New Zealand
MacDiarmid Institute for Nanotechnology and Advanced Materials, New Zealand

ARTICLE INFO

Article history:
Received 13 August 2008
Received in revised form 19 November 2008
Accepted 28 November 2008
Available online 14 December 2008

Keywords:
Pectin gels
Calcium association
Microrheology
Networks
Mechanical properties

ABSTRACT

Many of the functional attributes of pectin, whether in the plant cell wall or in engineered food materials, are linked to its gelling properties and in particular to its ability to assemble in the presence of calcium. Pectin's fine structure and local concentration relative to that of its cross-linking ion play a major role in determining resultant gel micro-structures, and consequently the mechanical and transport properties of pectin matrices. Recent studies have sought to probe the basic properties of such calcium-induced matrices, using a light scattering technique called diffusing wave spectroscopy (DWS). In addition to the low frequency mechanical behaviour, which provides information about the nature and density of cross-links, microrheological measurements carried out with DWS are able to determine the high frequency behaviour, which is closely linked to the response of the basic strands of the network. By using these microrheological measurements, two distinct regimes have been identified into which pectin gels appear to fall: one corresponding to the presence of semi-flexible networks, a generally accepted paradigm in biological gels, and another where flexible networks dominate. In order to explain the origin of these dramatically different networks, distinct assembly pathways have been proposed in which the relative importance of the free energy gained by association and the frictional barrier to polymeric re-arrangement during network formation can differ significantly. By manipulating the local environment in the plant cell wall it is possible that Nature makes full use of both of these network types for fulfilling different tasks; such as providing strain-hardening, maximizing local elastic properties or controlling macromolecular transport.

1. Introduction

The gelling abilities of pectin have been exploited by humans for a long time. The Romans learned from the Greeks that quinces, a pectin rich fruit, slowly cooked with honey would set when cooled, giving the recipe for Roman marmalade.[1] In 1825 Braconnot[2] wrote that pectin plays an important role in plant functions, and will have many applications in the art of the confectioner. Indeed, since then, research from plant biologists and food scientists on pectin has more than validated these two predictions, and currently pectin is of interest in a myriad of research areas including its possible medicinal benefits for the treatment of many diseases.[3–5]

Pectin is a ubiquitous polysaccharide of the plant cell wall, where it is known to play various mechanical roles; well-studied examples including controlling the mechanical properties of the pollen tube during growth[6] and mediating cell-cell adhesion.[7] Although the complete in vivo fine structure of this complex polysaccharide is still a matter of debate,[8,9] it is known that the homogalacturonan sections play the major role in determining its gelling abilities.[10] Homogalacturonan, which comprises the major part of commercially available pectins (typically >85%), is a linear co-polymer consisting of galacturonic acid residues and its methyl-esterified counterpart. For both the Golgi-synthesized biological substrate and for pectins extracted in the first stage of commercial processes, the relative quantity of the methyl-esterified residues (Degree of Methyl-esterification, DM) is high, and typically such polymers do not gel in presence of the main biological cross-linking agent, calcium cations.

In the plant cell wall, when calcium cross-linking is physiologically required, pectin is de-esterified in-muro by pectinmethylesterase (*p*-PME) enzymes. This de-esterification process takes place in the presence of a locally controlled concentration of its main binding ion, calcium. In contrast, for industrial applications, pectins extracted from apple pommace or citrus peels are typically de-esterified enzymatically or chemically before being sold, in order to increase calcium sensitivity and, when used in applications, are gelled with the subsequent introduction of Ca^{2+}. It is well known that the use of different chemical or enzymatic methods of de-esterification leads to different patterns in the intramolecular

* Corresponding author. Address: Institute of Fundamental Sciences, Massey University, Palmerston North, New Zealand.
E-mail address: m.williams@massey.ac.nz (M.A.K. Williams).

0008-6215/$ - see front matter © 2008 Elsevier Ltd. All rights reserved.
doi:10.1016/j.carres.2008.11.021

distributions of the liberated charged residues: pectinmethylesterase enzymes from land plants (*p*-PME) are known to produce a somewhat blocky pattern, while PMEs from fungus or a de-esterification carried out under alkali conditions will result in a random distribution of the exposed galacturonic acid residues. This large variability in the resultant polymeric fine structure gives ample opportunity to control the physical properties of resulting calcium-induced gels.

Indeed, a specific number of consecutive unesterified galacturonic acid residues are required to form a stable egg-box junction zone with calcium,[11,12] with estimates for this number varying between 8 and 15.[11,13] It is unsurprising then that, in general, a pectin sample with a blocky intramolecular DM distribution will tend to gel more easily, at an equivalent DM, when compared to a randomly patterned substrate. In order to characterize how 'blocky' a particular pectin is, two different degrees of blockiness (DB,[14] and DBabs[15]) have been defined, based on the quantity of short galacturonic acid oligomers which are liberated from the substrate by pectin degrading enzymes.

While the precise details of the binding of calcium ions by pectin is still an active area of research, the egg-box model[11] provides an excellent framework for its investigation; motivated by the success of this model in describing the association of calcium with alginate, another anionic polysaccharide with several similarities to pectin. More recently the interaction with calcium has been investigated by sophisticated molecular modelling techniques;[12] which, for both polymers, corroborated the idea of a two-stage process in the mechanism of calcium assembly, where the formation of strongly linked dimers is followed by the formation of weak inter-dimer associations. Such a multi-step mechanism has been verified experimentally for alginate by SAXS,[16] and in addition a third 'early' mono-complexation stage in the binding process has been suggested by calorimetric experiments,[17] corresponding to the interaction of Ca^{2+} with sugar residues from the same chain prior to egg-box formation. Although it is tempting to assume the same behaviour will be found for pectin systems, such direct comparisons currently lack relevant experimental evidence. At present, little SAXS data are published for pectin systems and while the calcium association processes in alginates and amidated pectins have been compared using isothermal titration calorimetry (ITC)[18], which is undoubtedly of great interest in its own right, the presence of the positively charged residues on the polymer backbone is expected to have a significant effect, rendering the prediction of behaviour for unamidated pectin difficult.

While ionic associations have been previously studied in dilute solution, in particular by electrochemical methods,[19,20] little is known about how the Ca^{2+} association in more concentrated solutions orchestrates the network assembly and how relevant dynamics might be harnessed in order to generate distinctly different functional networks. While state-of-the-art microscopy can generate high resolution images, it is still difficult to imagine the details of the self-assembly mechanism and the constitution of the network strands from the observation of the final pre-formed gel.[21–23] Furthermore, such high resolution images of networks require complex sample preparation that, while skilfully mastered by a few groups, yields direct imaging of network strand dynamics challenging.

An alternative way of obtaining information on the dynamics of the stress-bearing filaments of the network is to study the rheological behaviour of the induced materials. Bulk rheometers are routinely used to characterize visco-elastic materials, and indeed the linear mechanical properties of calcium-induced pectin gels have been investigated previously using such techniques.[24–26] However, classic rheometry offers limited information about the microstructure of the studied material owing to the relatively narrow frequency range accessible. It is typically limited to measuring low frequency mechanical properties, where studies potentially measure an elastic plateau and provide data primarily related to the cross-link density. In order to learn about the basic constitutive strands of the network, the study of the high frequency behaviour is essential. While recent advances have been made in the area of the development of high frequency rheometers,[27,28] microrheological techniques (MR)[29,30] and in particular a well-established multiple-light-scattering technique called diffusing wave spectroscopy (DWS) still surpass in this area. The aim of microrheology is to extract the rheological properties of soft materials from the motion of probe particles immersed in the material.[29,30] Passive microrheology is the simple study of the particle's thermal motion. It is a non-destructive technique and recovers the linear response of the material. For a viscoelastic fluid, the mean square displacement (MSD) of a probe particle will vary as a local power law $\langle \Delta r^2(\tau) \rangle \sim \tau^{\alpha}$ with $0 \leqslant \alpha \leqslant 1$ depending on the nature of the medium, and τ the observation time. The measured MSD can be linked to the viscoelastic properties, through a generalized Stokes–Einstein relation (GSER).

The first reported MR studies carried out on calcium-induced pectin gels have shown that these systems can exhibit the signatures of semi-flexible networks,[31,32] a paradigm for biological gels;[33] while more recent results have demonstrated that they can also behave as punctually cross-linked flexible networks.[34] Here we discuss a unifying framework encompassing the origin of both behaviours; show that the same pectin can be assembled so as to exhibit either kind of network, and tentatively propose a state diagram for the different modes of association of pectin chains.

2. Results and discussion

2.1. Characterization of the different regimes

Figure 1a shows the evolution of the mean square displacement (MSD) of embedded tracer particles versus lag time, tau, measured during the gelation of an enzymatically induced pectin gel, made as described in detail in the experimental section. In this system, the initially high DM pectin is incapable of binding the calcium ions (which are already present) into stable junction zones, until gelling is initiated by the release of calcium binding sites by added *p*-PME. This kind of gelation mechanism, where pectin is de-esterified in the presence of calcium, might present a reasonable mimic of gel formation in vivo. Remarkably, throughout the gel formation, the MSD at short times (high frequencies) scales with the time lag, tau, according to a power law with an exponent close to one half. This is significant as it is consistent with the predictions of Rouse theory,[35], that is, with the presence of a network made of *flexible* polymers. To further test this idea, the long time behaviour, which is linked to cross-links present in the network, was also studied. Assuming that the de-esterfication process follows Michaelis–Menton kinetics,[36] and that each substrate encounter yields a stable calcium binding site of the same average galacturonic acid block length, then the number of cross-links, N_C, will increase linearly with time after enzyme addition. Thereby, a plot of the low frequency MSD against time after enzyme addition is essentially equivalent to an investigation of how the network modulus (proportional to the reciprocal of the MSD) scales with the cross-linking density (proportional to the enzyme action time). Figure 1b shows such a plot of the MSD at 0.1 Hz versus time after enzyme addition, on double logarithmic axes, where a power law scaling with an exponent of -1.8 is evident. This is indeed consistent with previous work carried out on chemically cross-linked networks of *flexible* polymers.[34,37] To summarize: both the measured high frequency scaling of the MSD and it's dependence on the cross-link density at the low frequency are consistent with the presence of

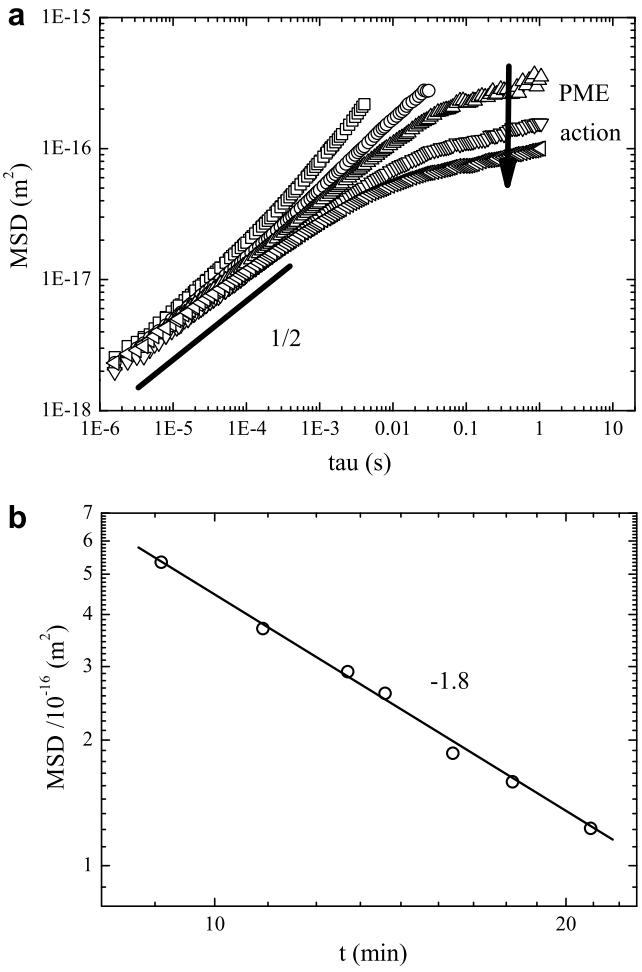

Figure 1. (a) The temporal evolution of tracer particle MSDs versus lag time, measured using DWS, during the formation of an enzymatically triggered pectin gel made as described in the text. The starting DM of the 1% w/w pectin solution is 78%, and the added calcium is equivalent to an R value of 0.3 for an equivalent DM of 60%. (b) The plateau value of the MSD/10^{-16} m^2, taken at 0.1 s from Figure 1(a), plotted against the time after introducing the enzyme, assumed to be proportional to the cross-link density N_C.

a network of randomly branched nature, in which the cross-links are short and punctual, and are bridged by flexible strands. It has been previously hypothesized[34] that these punctual cross-links are a result of the presence of short blocks of charged residues of the minimal length possible in order to form a stable calcium-mediated junction zone, which arise from *p*-PME action being curtailed by the presence of calcium, which facilitates intermolecular interactions that prevent the enzyme from acting again around the same position on the chain.

In order to characterize the pattern of ion-binding groups generated in such an experiment, and to provide further evidence that indeed the intra-molecular charge distribution generated by the enzyme might be modified by performing de esterification *in the presence of calcium*, two pectins were engineered from the same starting material. One was de-esterified by *p*-PME in presence of Ca^{2+} and one without Ca^{2+}, as detailed in the experimental section; where the pectin engineered in the presence of its binding ion was hypothesized to contain shorter blocks of acidic residues. While capillary electrophoresis (CE) gave a sample average DM of 62% for both pectins, the analysis of the products liberated when the samples were digested by a polygalacturonase, *endo*-PG II, revealed a notable difference in the average block length, as the digestion of the polymer made with *p*-PME in presence of calcium (PME62Ca) exhibited peaks in the electrophoregram corresponding to partially methylesterified oligomers, not present for the other pectin (PME62).[34] This is a strong sign that indeed *p*-PME de esterification in presence of Ca^{2+} does produce shorter galacturonic acid blocks when compared with the outcome of the *p*-PME action without Ca^{2+} present. These short blocks facilitate the formation of punctual cross-links and flexible networks.

Figure 2 shows the MSDs of embedded tracer particles, measured by DWS, for gels made by a slow release of calcium into solutions of the two polymer substrates engineered as described above, and detailed in the experimental section. The chosen conditions were a relatively high polymer concentration, 1% w/w, and an *R* value equal to 0.05, that is, a low calcium concentration. A low *R* value would be expected to result primarily in the formation of egg-box dimeric associations as suggested by SAXS[16] and calorimetric experiments[17] on the interaction between alginate and calcium. Typically alginate has a blocky distribution of its guluronic acid residues (unless specifically engineered to be alternating[38]), so it might be expected that blocky pectins would exhibit similar interactions with calcium. It is clear that the slope of the MSD at high frequencies (short times) on the double logarithmic plot again follows the Rouse model,[35,39] as shown in Figure 1a, scaling with time lag with a power law with an exponent of ½ for both kinds of pectin. This is again consistent with the formation of short dimeric cross-links acting as punctual chemical cross-links in a solution of flexible polymers. While this was expected for the PME62Ca sample containing short charged blocks capable of forming dimeric egg-box zones, these results also suggest that PME62 pattern is also made of relatively short blocks, despite the fact that the action of *p*-PME enzymes is often described (at least for substrates modified to low DM) as producing very blocky charge distributions. This is further evidence that the degree of processivity of *p*-PMEs may in fact be relatively small,[40,41] typically yielding patterns of unesterified galacturonic acid residues being described by numerous relatively short blocks at moderate to high DM values, with longer blocks emerging at higher degrees of de-esterification, or from pectins with a very high initial degree of methylesterification. Modelling the de-esterification process itself forms part of ongoing work.

The analysis of the 'plateaus' of the MSDs seen at longer times in Figure 2 is also consistent with the presence of shorter blocks for the pectin de-esterified in the presence of calcium, PME62Ca, as the MSD plateau is lower than that obtained from the gel made with the PME62 sample, a sign of a higher cross-link density. As the (limiting) Ca^{2+} concentration is the same in both gels, this implies that the length of the calcium junction zones is smaller for the gel made with PME62Ca. Indeed, this result has much to say about the strategy for maximizing the elastic properties of gels made from pectins of a fixed DM: by generating a fine structure in which each calcium-binding junction zone is only the minimum length possible for ensuring stability at a prerequisite temperature, it is possible to maximize the number of such connections. For flexible networks of this type, any further increase in the length of these junctions simply wastes charged residues that could be utilized elsewhere. While locally terminating *p*-PME action by the presence of calcium ions is an effective way of generating such fine structures containing the minimum calcium-interacting lengths of galacturonic acid residues, *p*-PME itself also seems capable of creating short (but long enough) blocks, as long as the starting substrate is not of extremely high DM.

The gradient of the long-time 'plateau' is another interesting aspect of the data shown in Figure 2: the MSD of the tracer particles in the PME62Ca gel can be seen to be approximately flat at long times, clearly not the case for the PME62 material. While the relative constancy of the MSD in the former can be seen as an indication of a more rubber-like truly elastic network, the latter evidently does not reach a state that is totally percolated by

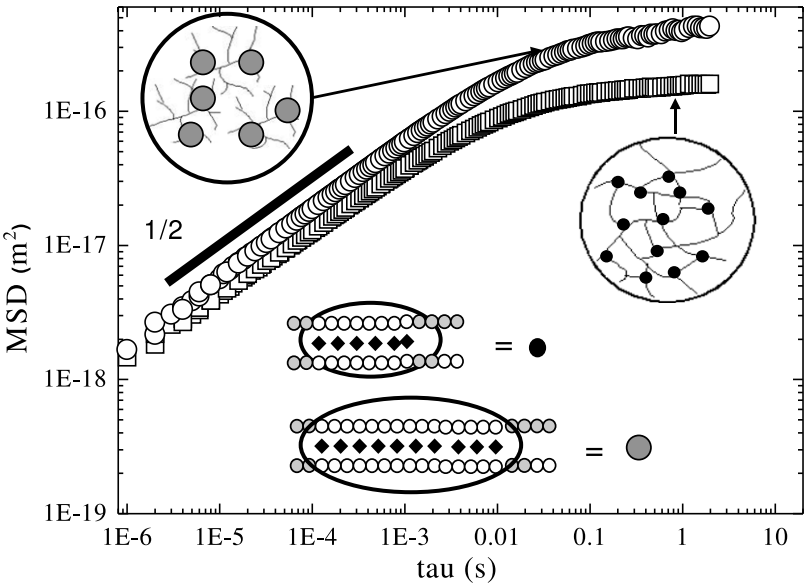

Figure 2. The resulting MSDs obtained from probe latex particles embedded in gels formed by the slow release of calcium (as described in the experimental section) for two pectin samples of DM 62% which have been obtained by de-esterification with *p*-PME in the presence (squares) and absence of Ca^{2+} (circles), respectively. The polymer concentration is 1% w/w, and the calcium concentration is equivalent to an *R* value of 0.05. The PME62 sample (containing longer but less numerous calcium junction-zone forming runs) is more characteristic of a branched polymer solution, while the PME62Ca sample (containing shorter but more numerous charged calcium junction-zone forming runs) has a higher cross-link density and can be viewed more as a rubber-like network.

long-lived cross-links, and is better described as a solution of highly branched high molecular weight flexible polymers, with the slow reptation of these high molecular weight assemblies explaining the slight relaxation at longer times. It would be reasonable then to estimate that the cross-link density required for percolation lies between that exhibited by these two systems. In order to explain the appearance of a percolated network, we can estimate that each PME62Ca chain has a minimum of two cross-links formed with calcium, and as the *R* value used limits those sites actually bound to be around one quarter of those potentially available, this indicates that around eight regions of potential calcium binding were introduced into each chain by the deesterification process that reduced the DM by some 16% (78→62%). Ignoring the original randomly distributed unesterified regions in the starting high DM pectin owing to the low probability of sufficiently long bare galacturonic acid runs to be able to form stable cross-links existing, and using an average degree of polymerization of some 350 residues, a rough estimate of the length of a junction zone of about seven residues is found ($(16/100) \times 350/8$). Interestingly, this is indeed close to other estimates of the minimum number of consecutive acidic residues necessary to form a stable junction zone.[13] As noted, the PME62 sample has a larger long-time displacement and hence smaller modulus by a factor of around two, and assuming now that this system is close to percolation, this roughly reflects the presence of half the junction zones; or equivalently a doubling of the estimated junction zone length to approximately 14 residues, again reasonably close to emerging ideas of *p*-PME processivity.

Interestingly, all the systems studied in this 'flexible regime' exhibit behaviour in stark contrast to that found in previous work,[31] in which microrheological studies were carried out on pectin gels which clearly showed the signatures of semi-flexible networks theories.[42,43] The main predictions of these theories are a power law scaling of the high frequency MSD with an exponent of ¾ with lag time, and a scaling of the plateau MSD at long time with an exponent of 1.4 with polymer concentration. The extensively studied pectin sample used in these previous studies[31] was of a lower DM (50%), was considered to have a very blocky intramolecular pattern of unesterified residues owing to the fact it was de-esterified by *p*-PME and was subsequently gelled after de-esterification, using a controlled release of calcium. At first glance the different behaviour of that system compared to that shown here in Figures 1 and 2 might be simply assigned to fine-structure differences, that is, that the semi-flexible regime might only be manifest by pectins containing unesterified blocks of significant length, where long calcium bound dimers form the actual network strands themselves, rather than simply connecting together more flexible filaments. To attempt to test such a hypothesis and to better understand the origins of the different regimes, further pectin gels were assembled from the two polymers described above, PME62 and PME62-Ca, but now at lower polymer, and higher calcium, concentrations, in order to match the conditions found in the previous semi-flexible network study. (These conditions had evolved largely as a practical response to restricting the modulus and gelation rate of systems of very blocky pectins while still creating percolated networks.) The results are shown in Figure 3a, and perhaps surprisingly a power law scaling of the MSD with lag time with an exponent of ¾ was observed at short times, for both pectins. Furthermore, the MSD of both gels is very similar over the whole frequency range, a sign that the density of the semi-flexible filaments, as well as the cross-link density, is about the same for both gels.

To further corroborate the existence of a *semi-flexible* regime, even for the polymers possessing a fine structure that so convincingly illustrated *flexible* network behaviour in Figure 2, DWS experiments were carried out on the PME62 gels made with a slow release of calcium, for different polymer concentrations. As depicted in Figure 3b, the familiar ¾ high frequency scaling of the tracer MSD with lag time is found for concentrations ranging from 0.4% to 0.8% w/w, and indeed in this region the MSD plateau value scales reasonably well with the polymer concentration with a power law of −1.4 (Fig. 3b Inset). These results agree well with predictions based on the presence of a semi-flexible network, although the pectins used are made of relatively short charged blocks. It seems unlikely then that the actual semi-flexible filaments could be only dimeric junction zones as initially postulated,[31] suggesting the possible assembly of stiff network strands with a certain chain multiplicity.

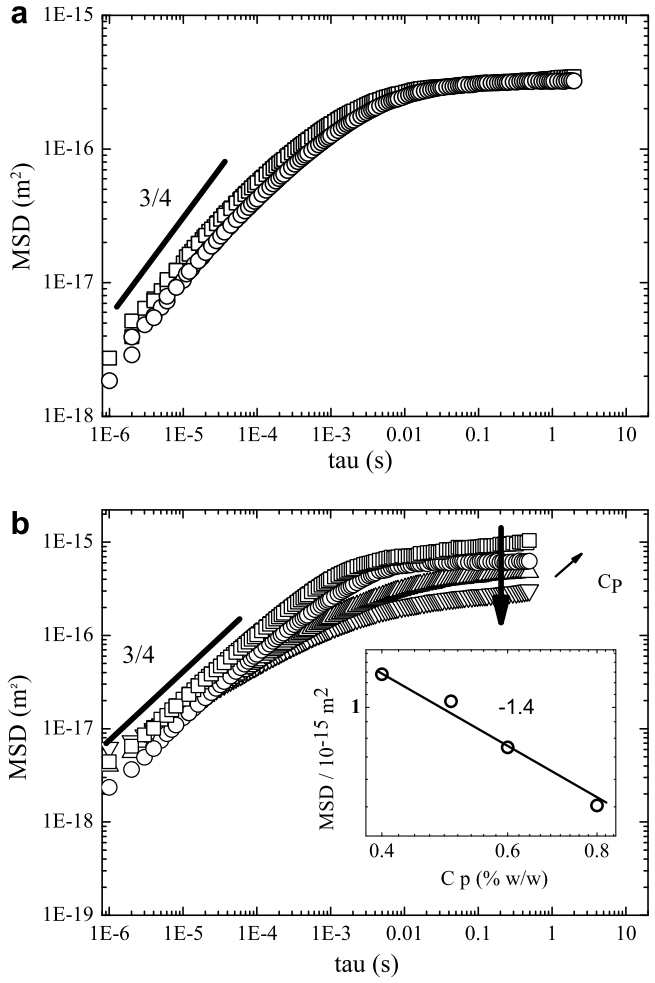

Figure 3. (a) The resulting tracer particle MSDs obtained by DWS from gels created by the slow release of calcium (as described in the experimental section) from PME62 (squares) and PME62Ca (circles), with polymer concentrations of 0.5% w/w and $R = 0.25$ ($R_{eff} = 0.6$; see Eq. 1). (b) The resulting MSDs obtained from DWS for the PME62 for $R = 0.25$ ($R_{eff} = 0.6$; see Eq. 1), as in (a), but here for concentrations ranging from 0.4% to 0.8% w/w. Inset: The plateau value of the MSD/10^{-15} m^2, taken at 0.1 s, plotted against the pectin concentration (% w/w).

While relating the persistence length of formed semi-flexible filaments to their chain multiplicity is not trivial, it is possible that individual dimers are not, in fact, sufficiently stiff so that their bending energy contributes significantly to their resistance to deformation. Although in detail how the stiffness, apparent charge density parameter and preferred helical conformation of calcium-assembled filaments vary with bundle multiplicity is unknown, assuming an increasing bending rigidity with an increasing number of incorporated chains seems a reasonable working hypothesis. In fact, there is a precedent for the existence of higher order multiple chain associations at high concentrations of calcium. In alginate systems, which we have argued are a reasonable analogue of blocky pectin systems, previous studies[16,17] observed that at *high calcium concentrations*, there was indeed a lateral association of egg-box dimers, as also suggested by modelling.[12] While these studies were carried out at relatively low alginate concentration where such stiff filaments would fail to percolate, in our semi-dilute systems these filaments form a topologically entangled semi-flexible network, yielding the observed concentration dependence, with light cross-linking by longer lived transient lateral associations providing the long-time dependence.

However, in conditions of higher concentrations of polymer and low concentrations of calcium, such as the systems studied in Figure 2, the same polymeric fine structure yields flexible networks. There is some evidence[16,17] from dilute systems that multiple chain associations simply do not form below a certain concentration of calcium, presumably because they are simply out-competed by the formation of egg-box type dimers. Additionally, even at higher concentrations of calcium, it seems reasonable to argue that in semi-dilute and concentrated systems, extensive lateral chain associations that would otherwise yield semi-flexible filaments could be prohibited because the high degree of mobility required for the polymers to rearrange into such configurations is curtailed. The slower reptative dynamics characterizing the systems ability to rearrange at higher concentrations owing to topological restrictions and possible transient lateral interactions involving limited chain lengths, means that as small amounts of calcium are introduced and minimum-length calcium-binding junction zones are formed, 'spot-welds' are introduced which dynamically trap the entangled polymer solution in a state where the stress-bearing elements are flexible polymers linked by short, punctual, dimeric cross-links.

2.2. State diagram

How different conditions ultimately yield different network regimes; characterized by the way the calcium-induced associations either (i) pin flexible entangled systems with punctual cross-links or (ii) drive rearrangement and bundling of multiple polymers into semi-flexible filaments, can be summarized in a state diagram. Clearly such a diagram will contain regions corresponding to basic dimeric association and lateral association of the initial dimers.

An initial somewhat pragmatic approach to such a diagram would be to plot the described regions as a function of polymer concentration and R value. However, the traditionally calculated R value appears of questionable use as a unifying parameter able to cope with fine structures differences, counting, as it does, the quantity of calcium relative to the *total* number of charged galacturonic residues, despite the fact that it is often clear that a substantial portion of these residues can never form stable egg-box junction zones, owing to the nature of the intramolecular charge distribution. When searching for universal behaviour resulting from calcium binding, it is possible that another parameter, R effective or R_{eff}, might prove to be more useful; defined as a ratio in the spirit of the well-known *R value*

$$R_{eff} = \frac{2 \cdot [Ca^{2+}]}{[COO^-]_{eff}} \quad (1)$$

but where $[COO^-]_{eff}$, rather than counting all galactuonic acid, is the quantity contained in blocks of consecutive unesterified residues longer than a defined amount, specifically that amount required to bind calcium into a stable junction zone. This definition of R_{eff} could readily be used for pectins possessing blocky or indeed random intramolecular distributions of methylesterification, but strictly its calculation requires knowledge of a precise minimum number of consecutive residues required in order to form a stable junction zone at the temperature of interest. At present, experimental estimates of this number range between 8 and 15,[11,13] consistent with our estimates from this work.

However, for the pectins used in this study this lack of detailed knowledge required to calculate the proposed R_{eff} can be circumvented by making two assumptions (i) that the initial 78% DM pectin (that was subsequently deesterified with *p*-PME to produce the investigated samples) does not contribute any residues to this ratio, that is, the probability of having even eight consecutive unesterified residues in the starting material is negligible and (ii) that owing to the *raison d'être* of *p*-PME all the residues that were introduced by its deesterification of the starting substrate do contribute to the ratio. Thus, for the systems investigated here we have

$$R_{eff.PME} = \frac{2 \cdot 100 \cdot [Ca^{2+}]}{\Delta DM \cdot [GalU]} \quad (2)$$

where ΔDM (%) is the decrease in DM generated by *p*-PME de-esterification, and *[GalU]* the quantity of the galacturonic residues.

Figure 4 shows a proposed state diagram that has been experimentally mapped out, using this definition of R_{eff}, for gels made from the PME62 pectin, with boundaries estimated at the demarcation of the different regimes. Several key features of the arguments elaborated in the text are evident. For example, for relatively high calcium concentrations and low enough polymer concentration, lateral association of the primary dimers, permitted due to high system mobility, results in multiple chains assembling into semi-flexible filaments. In dilute solution, such filaments have previously been reported as multiple associated chains, as described for alginate in ITC experiments at high *R* values[17] (Region (a)). At higher polymer concentrations, percolated semi-flexible networks based on these filaments are formed, as observed in microrheological studies described previously and herein (Region (b)). As the polymer concentration is increased still further, the system mobility is reduced significantly, and extensive lateral association of the dimers is dynamically forbidden even at high calcium concentrations, resulting in flexible networks in which the polymers are dynamically pinned (Region (c)). For low Ca^{2+} concentrations, the scheme is simpler with both the dilute and semi-dilute regimes containing predominantly dimeric egg-box junctions that are manifest either as analogous chain associations to those detected in ITC experiments of alginate (Region (d)) or yield cross-linked flexible networks, respectively, (Region (e)).

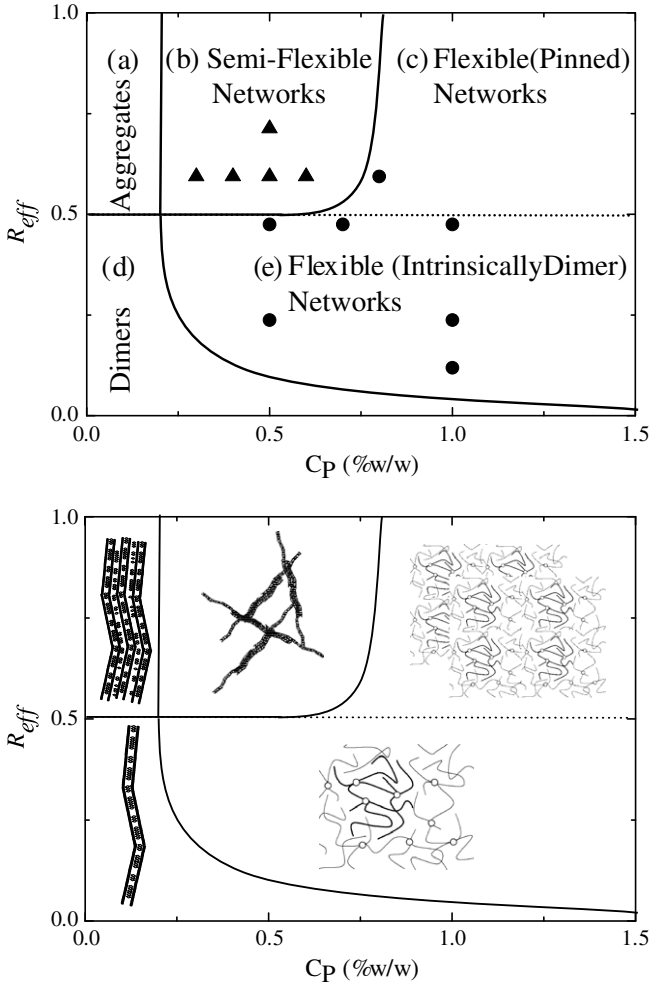

Figure 4. A proposed state diagram for PME62. (Top) The points shown correspond to the results of the DWS experiments presented in Figures 2 and 3, plus additionally measured points (raw data not shown). Triangles are plotted where, at that polymer concentration and R_{eff} value, semi-flexible signatures were found; and similarly circles denote systems where the experimentally determined signatures of flexible networks were observed. The different sketched regions (a)–(e) are described in Section 2.2. (Bottom) Schematic of the proposed state diagram.

According to our microrheology experiments the calcium concentration below which we cannot observe semi-flexible network behaviour is approximately at $R_{eff} = 0.5$, and it is indeed interesting to note that it has been proposed that this is the limit when all the possible dimers are formed in alginate,[16] with the lateral association of these dimers occurring at higher R_{eff} (when not dynamically constrained). For alginate, which typically has a blocky pattern of ion-binding groups, *R* would be equivalent to R_{eff}. Other work also found that for alginates inter-dimer associations occurred for *R* values higher than 0.55,[17] close to the boundary proposed here. By using R_{eff} as the parameter embodying this relative calcium concentration, this boundary should be more robust to changes of pectin fine structure, although randomly distributed patterns of methylesterification are worthy of investigation and form part of ongoing work. The other significant boundary is found upon increasing the polymer concentration, signalling the point at which the polymeric mobility in the embryonic networks is reduced (owing to extensive entanglement and also pinning by the initial bound calcium) to an extent where further network rearrangements and extensive lateral aggregation are not possible. This point will be linked primarily to a specific entanglement or cross-link density, capable of modifying the system dynamics sufficiently to prevent substantial rearrangements. As such, the average block length of the calcium binding sugars would be expected to modify this limit, where increasing the block length might be expected to move the boundary towards higher polymer concentrations at a chosen R_{eff} value. The influence of pectin fine structure on such a state diagram is proposed in Figure 5.

It is expected that ultimately, as more information becomes available on the energetics of calcium binding and more experimental techniques are brought to bear, in an effort, for example, to directly measure the local polymer mobility during gelation, that such fine structure dependent state diagrams might be collapsed onto a universal plot in which the physics is embodied in the relative importance of the free energy gained by associations of various types and the frictional barriers to polymeric rearrangement.

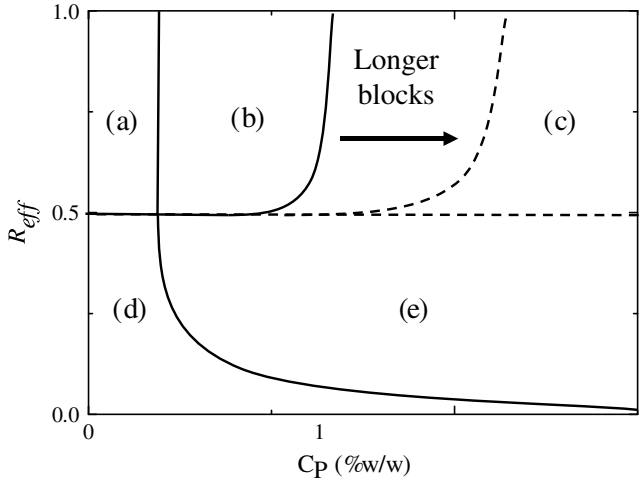

Figure 5. Proposed evolution of the suggested state diagram depending of the pectin fine structure: charged residues distributed in short blocks (bold), long blocks (dash). The regions (a)–(e) are the same as in Figure 4.

3. Conclusion

Recent microrhelogical studies have been offering insights into the fundamental nature of pectin gels by giving unprecedented access to the high frequency mechanical properties, which reflect the properties of the network strands; in addition to the low frequency data which act as a valuable indicator of more global network properties such as the cross-link density. While initial studies of the dynamic–mechanical response of ionotropic gels made from extracted pectins, whose primary structure was modified in vitro, exhibited behaviour indicative of semi-flexible polymer networks, (the high frequency moduli scale with $\omega^{3/4}$, and the dependence of the elastic plateau on cross-link density follows $N_C^{1.4}$); subsequently studied systems in which *p*-PME was used to liberate calcium binding sites on initially highly methylesterified pectin in the presence of calcium-ions clearly showed the signatures of chemically cross-linked networks of flexible polymers (the high frequency moduli scale with $\omega^{1/2}$, and the dependence of the elastic plateau on cross-link density follows $N_C^{1.8}$).

In this work, microrheological studies have been performed on calcium-induced gels made from two different high DM (62%) blocky pectins with controlled fine structures, one engineered to contain the shortest possible blocks capable of binding calcium into a stable junction zone, and one with longer (though still short) blocks. It was found that both of these fine structures were able to produce gels exhibiting behaviour characteristic of *either* the semi-flexible or flexible regime, depending on the polymer concentration and the relative calcium concentration. Thereby, using polymer concentration and a newly defined parameter, the effective *R* value, R_{eff} (which quantifies the calcium concentration relative to only the number of charged galacturonic acid residues which can potentially bind Ca^{2+} *into a stable cross-link*) a state diagram has been mapped out describing regions of the parameter space where each behaviour might be expected. Furthermore, the origin of these dramatically different networks has been rationalized with recourse to basic physical principles into a common framework in which the relative importance of the free energy gained by association and the frictional barrier to polymeric re-arrangement during network formation play significant competing roles.

The ability of plants to control local polymer and ion concentration suggests that both semi-flexible *and* flexible networks may be relevant in vivo, and could provide different functionalities. For example, while the semi-flexible networks previously observed are more likely to exhibit strain hardening, the flexible networks described herein optimize the elasticity of calcium-bonded networks by utilizing a specific pattern of short ion-binding blocks. It is also interesting to consider that these network types will have vastly different transport properties, and the ability to select between these may well play a role in controlling the porosity of the cell wall.

4. Materials and methods

4.1. Materials

Pectin ($M_w \sim 30$–100 kDa), extracted from apple pomace, was purchased from Fluka Biochemika (Sigma Aldrich, Switzerland). The sample average DM of this sample and all others produced by modification were determined using capillary zone electrophoresis (CE) as previously described.[44,45]

Pectinmethylesterase of plant origin (*p*-PME) [EC 3.1.1.11] purchased from Sigma Aldrich (P5400) was used in order to remove methylester groups from the starting pectin substrate.[46] Stock solutions of the enzyme were prepared by dissolving 0.01 g of dried *p*-PME in 20 mL in Milli-Q water, and were stored at −20 °C in Eppendorf tubes. Aliquots were thawed prior to conducting experiments and used immediately. This *p*-PME has a peak of activity at pH 7.5, and this was maintained throughout our experiments with the use of a buffer, as described below.

Polygalacturonase [EC 3.2.1.15] was used to digest the polymeric substrates in order to verify differences in the intramolecular distribution of the calcium binding groups. The enzyme was kindly provided by Jacques Benen from the University of Wageningen. It is a pure endo-PG II isoform from *Aspergillus Niger*[47] and has an absolute requirement for the sugar residues in the active site to be unesterified in order for the chain to be severed, which yields the degradation pattern methylester-sequence dependent. The pectin substrates were digested for 24 h at 30 °C. A 1 mL solution of substrate at a concentration of 0.5% w/w and pH 4.2 (acetate buffer 50 mM) was incubated with 20 μl of enzyme solution (0.094 mg/mL protein). At the end of the reaction, the enzyme was denatured at 90 °C for 3 min.

$CaCO_3$ powder with a mean particle diameter of 1 μm was kindly provided by Provencale s.a., Avenue Frédéric Mistral, 83172 Brignoles Cedex, France.

Glucono-δ-lactone (GDL) was purchased from Fisher Scientific, Bishop Meadow Rd, Loughbourough, LE11 5RG, UK.

Latex particles of diameter 465 nm (2.62% w/v stock solutions) were purchased from Polyscience Inc. (Warrington, PA).

4.2. Pectin fine structure engineering

Pectin solutions of 1% w/w were made by dissolving the pectin powder in a 50 mM HEPES buffer, adjusted to pH 7.5 with NaOH. A $CaCl_2$ salt was then added for the *p*-PME de-esterification in the presence of Ca^{2+}, or the equivalent quantity of Milli-Q water when the de-esterification was performed without Ca^{2+}. The quantity of added $CaCl_2$ was in slight excess over the final quantity of de-esterified residues, in order to ensure that every created block capable of binding calcium into a stable junction did so at any stage of the reaction. Enzyme solution (0.5 mL) was then mixed into 30 mL of the desired solution containing pectin, and the mixture left at 20 °C for a chosen time, depending on the final DM decrease required and on the rate of the de-esterification processes. Assuming the enzymes followed a simple Michaelis–Menton model[36] and were in the linear section of the product production curve (which was monitored independently using NMR to follow the liberation of methanol), preliminary experiments were used to determine the rate of DM decrease as −4%/h for the *p*-PME de-esterification without Ca^{2+}, and −5.8%/h in presence of Ca^{2+}.

Thus, the *p*-PME action could be stopped after a pre-requisite time in order to achieve a desired final DM. This was carried out by decreasing the pH and subsequently heating the solution at 80 °C for 5 min to denature the enzyme. For a final DM of 62%, this was performed easily when no calcium was present, although a strong mixing was necessary to break the gel formed in presence of calcium.[34] Subsequently, the modified polymers were extracted by dialysing the sample twice under acidic conditions against a 10^{-2} M solution of HCl, and finally twice against Milli-Q water. The dialyzed solutions were freeze dried and the engineered polymers recovered and stored dry. The recovered pectin samples had their fine structures analyzed by capillary electrophoresis (CE[46]), characterizing the sample average degree of methyl-esterification of the pectin, and providing qualitative information about the distribution of the acidic residues by analyzing the *endo*-PGII-digest products.[48,49]

4.3. Enzymatically induced pectin gels

For MR experiments, stock pectin solutions of 1.8% w/w were prepared by dissolving the pectin powder in a 50 mM HEPES buffer made with Milli-Q water, adjusting to pH 7.5 with NaOH, and

stirring for 1 h. Subsequently, desired volumes of a $CaCl_2$ salt solution and of the stock bead solution were added in order to achieve a final concentration of 0.8% of microspheres in solution. As described in Section 4.2, the quantity of $CaCl_2$ was again in excess when compared to the final quantity of de-esterified residues. Finally the sample was mixed with the desired volume of water, in order to reach a final polymer concentration of 1% w/w. As the starting pectin was of a high DM, it did not gel in the presence of the added Ca^{2+}. Immediately prior to loading the solution in the test chamber, 25 μL of enzyme solution was added for 1.5 mL of pectin solution, and mixed for 5 min before starting the measurements.

4.4. Calcium-induced gels

Ionotropic pectin gels were also obtained by slowly releasing calcium ions into buffered (HEPES 50 mM) solutions of pectin with fine structures determined by prior enzyme processing,[50] containing 0.8% of 465 nm latex beads. The appropriate amounts of pectin and bead stock solutions were mixed and stirred, and immediately prior to loading into appropriate test cells a salt solution was added, the final mixing of which achieves the final desired concentration of all components of the system. This aqueous salt solution was composed of $CaCO_3$ and GDL. The GDL hydrolyzes with time, releasing protons that solubilize calcium ions from the $CaCO_3$. These components were introduced as powders into water, quickly mixed, and added to the pectin-bead solution as quickly as possible, in order to avoid significant calcium release before mixing with pectin. The quantity of $CaCO_3$ added determines the R_{eff} value, described in the text, which can, by controlling the amount and extent of interchain association, be varied to tune the elasticity of the material. R_{eff} is related to the R value, $R = 2\times[Ca^{2+}]/[COO^-]$, which is commonly used to describe the calcium binding to pectin and alginate, as described in the main text. A stoichiometric ratio of GDL, $[GDL] = 2 \times [Ca^{2+}]$, was used in order to have minimal effect on the sample pH. After the addition of the salts, the final prepared solution was stirred for a few minutes, and the samples were loaded into the appropriate test cell and left overnight.

4.5. Microrheology

For a viscoelastic fluid, the mean square displacement (MSD) of a probe particle will vary as a local power law $\langle \Delta r^2(\tau)\rangle \sim \tau^{\alpha}$ with $0 \leqslant \alpha \leqslant 1$ depending on the nature of the medium, and τ is the observation time. The measured MSD can be linked to the viscoelastic properties, through a generalized Stokes–Einstein relation (GSER),[51] with the caveats that the fluid is incompressible and the boundary non-slip, such that

$$\hat{G}(s) = \frac{k_B T}{\pi a s \langle \hat{\Delta} r^2(s)\rangle} \tag{3}$$

with $\hat{G}(s)$ is the shear modulus in the Laplace space, s the Laplace frequency and $\langle \hat{\Delta} r^2(s)\rangle$ the Laplace transform of the MSD. However, valuable physical insight can be gained purely from the behaviour of the MSD, with various well-established theories making distinct predictions based on different microstructural models.

The DWS apparatus used in this study has been fully described previously.[52] The samples were contained in glass cells of width 10 mm, height 50 mm and path length L of 4 mm, and were illuminated with a 35 mW He–Ne Melles-Griot laser operating at wavelength $\lambda = 633$ nm. The laser beam was expanded to approximately 8 mm on the surface of the cell. The transmitted scattered light was detected using a single-mode optical fibre (P1-3224-PC-5, Thorlabs Inc., Germany). The optical fibre was connected to a Hamamatsu HC120-08 PMT photomultiplier tube module, and the intensity autocorrelation functions of the scattered light were obtained using a Malvern 7132 correlator. Tests were run for 10 min to ensure low noise intensity autocorrelation functions.

For an expanded beam mode, the field autocorrelation function is $g_1(t)$ and is obtained from the measured intensity autocorrelation function $g_2(t)$ using the Siegert equation $g_2(t) = 1 + \beta g_1^2(t)$, where β is a constant depending on the instrument. In the transmission geometry, the field autocorrelation function is given by[53]

$$g_1(t) = \frac{\frac{L/l^*+4/3}{z_0/l^*+2/3}\left\{\sinh\left[\frac{z_0}{l^*}\sqrt{k_0^2\langle\Delta r^2(\tau)\rangle}\right] + \frac{2}{3}\sqrt{k_0^2\langle\Delta r^2(\tau)\rangle}\cosh\left[\frac{z_0}{l^*}\sqrt{k_0^2\langle\Delta r^2(\tau)\rangle}\right]\right\}}{\left(1+\frac{8t}{3\tau}\right)\sinh\left[\frac{L}{l^*}\sqrt{k_0^2\langle\Delta r^2(\tau)\rangle}\right] + \frac{4}{3}\sqrt{k_0^2\langle\Delta r^2(\tau)\rangle}\cosh\left[\frac{L}{l^*}\sqrt{k_0^2\langle\Delta r^2(\tau)\rangle}\right]} \tag{4}$$

where l^* is the scattering mean free path, z_0 the penetration depth (assumed here to equal l^*), $k_0 = 2\pi n/\lambda$ and L the sample thickness (4 mm here). l^* is obtained by performing an experiment on a water sample using 0.8% of latex beads, and fitting l^* using the accepted viscosity. Subsequently l^* for future samples is obtained by scaling the value obtained for water, based on the change in transmitted intensity when the sample is introduced, compared to the water experiment. It is known that for non-absorbing slabs of thickness L, the transmitted intensity is directly proportional to $(5l^*/3L)(1 + 4l^*/3L)$, so that by measuring the change in transmittance, the change in l^* can be calculated.[53,32] Once l^* is determined, the MSD can be obtained from the experimental correlation functions by inverting the above expression for $g_1(t)$ with a zero-crossing routine. That is, for each time point, the value of $\langle \Delta r^2(\tau)\rangle$ that is required in order for Eq. 4 to match the experimentally measured $g_1(t)$ is determined.

Acknowledgements

The authors gratefully acknowledge the financial support from the MacDiarmid Institute (New Zealand) for the PhD scholarship of Romaric R. Vincent. Many thanks to Yacine Hemar for valuable discussions and help with the DWS experiment, and thanks to Aurélie Cucheval for help with the polymer modifications and characterization.

References

1. Apicius, *De re coquinaria, 4th century AD*. Translation: *Apicius, The Roman cookery book tr. Barbara Flower*, Elisabeth Rosenbaum. London: Harrap, **1958**.
2. Braconnot, H. *Annales de chimie et de physique-Ann. Chem. Phys.* **1825**, *28*, 173–178.
3. Pilnik, W. In *Gums and Stabilizers for the Food Industry*; Phillips, G. O., Williams, P. A., Wedlock, D. J., Eds.; Oxford University Press: Oxford, 1990; pp 313–326.
4. May, C. D. In *Thickening and Gelling Agents for Food*; Imeson, A., Ed.; Blackie Academic and Professional: London, 1997. pp 124–152.
5. Jackson, C. L.; Dreaden, T. M.; Theobald, L. K.; Tran, N. M.; Beal, T. L.; Eid, M.; Gao, M. Y.; Shirley, R. B.; Stoffel, M. T.; Kumar, M. V.; Mohnen, D. *Glycobiology* **2007**, *17*, 805–819.
6. Parre, E.; Geitmann, A. *Planta* **2005**, *220*, 582–592.
7. Willats, W. G. T.; Orfila, C.; Limberg, G.; Buchholt, H. C.; van Alebeek, G. J. W. M.; Voragen, A. G. J.; Marcus, S. E.; Christensen, T. M. I. E.; Mikkelsen, J. D.; Murray, B. S.; Knox, J. P. *J. Biol. Chem.* **2001**, *276*, 19404–19413.
8. Willats, W. G. T.; Knox, P.; Mikkelsen, J. D. *Trends Food Sci.Technol.* **2006**, *17*, 97–104.
9. Vincken, J. P.; Schols, H. A.; Oomen, R. J. F. J.; McCann, M. C.; Ulvskov, P.; Voragen, A. G. J.; Visser, R. G. F. *Plant Physiol.* **2003**, *132*, 1781–1789.
10. Yapo, B. M.; Lerouge, P.; Thibault, J. F.; Ralet, M. C. *Carbohydr. Polym.* **2007**, *69*, 426–435.
11. Powell, D. A.; Morris, E. R.; Gidely, M. J.; Rees, D. A. *J. Mol. Biol.* **1982**, *155*, 517–531.
12. Braccini, I.; Perez, S. *Biomacromolecules* **2001**, *2*, 1089–1096.
13. Liners, F.; Thihbault, J. F.; Vancustem, P. *Plant Physiol.* **1992**, *99*, 1099–1104.
14. Daas, P. J. H.; Meyer-Hansen, K.; Schols, H. A.; De Ruiter, G. A.; Voragen, A. G. J. *Carbohydr. Res.* **1999**, *318*, 135–145.
15. Daas, P. J. H.; Voragen, A. G. J.; Schols, H. A. *Carbohydr. Res.* **2000**, *326*, 120–129.
16. Stokke, B. T.; Draget, K. I.; Smidsrød, O.; Yuguchi, Y.; Urakawa, H.; Kajiwara, K. *Macromolecules* **2000**, *33*, 853–1863.

17. Fang, Y. P.; Al-Assaf, S.; Phillips, G. O.; Nishinari, K.; Funami, T.; Williams, P. A.; Li, L. B. *J. Phys. Chem. B* **2007**, *111*, 2456–2462.
18. Fang, Y. P.; Al-Assaf, S.; Phillips, G. O.; Nishinari, K.; Funami, T.; Williams, P. A. *Carbohydr. Polym.* **2008**, *72*, 334–341.
19. Kohn, R. *Pure Appl. Chem.* **1975**, *42*, 371–397.
20. Ralet, M. C.; Crepeau, M. J.; Buchholt, H. C.; Thibault, J. F. *Biochem. Eng. J.* **2003**, *16*, 191–201.
21. Kirby, A. R.; Gunning, A. P.; Morris, V. J. *Biopolymers* **1996**, *38*, 355–366.
22. Lofgren, C.; Walkenstrom, P.; Hermansson, A. M. *Biomacromolecules* **2002**, *3*, 1144–1153.
23. Fischman, M. L.; Cooke, P. H.; Chau, H. K.; Coffin, D. R.; Hotchkiss, A. T. *Biomacromolecules* **2007**, *8*, 573–578.
24. Ström, A.; Ribelles, P.; Lundin, L.; Norton, I.; Morris, E. R.; Williams, M. A. K. *Biomacrolecules* **2007**, *8*, 2668–2674.
25. Durand, D.; Bertrand, C.; Clark, A. H.; Lips, A. *Int. J. Biol. Macromol.* **1990**, *12*, 14–18.
26. Clark, A. H.; Farrer, B. D. *Food Hydrocolloid* **1996**, *10*, 31–39.
27. Crassous, J. J.; Regisser, R.; Ballauff, M.; Willenbacher, N. *J. Rheol.* **2005**, *49*, 851–863.
28. Willenbacher, N.; Oelschlaeger, C.; Schopferer, M.; Fischer, P.; Cardinaux, F.; Scheffold, F. *Phys. Rev. Lett.* **2007**, *99*, 068302.
29. Gardel, M. L.; Valentine, M. T.; Weitz, D. A. In *Microscale Diagnostic Techniques*; Breuer, K., Ed.; Springer, 2005.
30. Waigh, T. A. *Rep. Prog. Phys.* **2005**, *68*, 685–742.
31. Vincent, R. R.; Pinder, D. N.; Hemar, Y.; Williams, M. A. K. *Phys. Rev. E* **2007**, *76*, 031909.
32. Williams, M. A. K.; Vincent, R. R.; Pinder, D. N.; Hemar, Y. *J. Non-Newtownian Fluid Mech.* **2008**, *149*, 63–70.
33. Levental, I.; Georges, P. C.; Janmey, P. A. *Soft Mat.* **2007**, *3*, 299–306.
34. Vincent, R. R.; Cucheval, A.; Hemar, Y.; Williams, M. A. K. *Eur. Phys. J. E.*, in press.
35. Rouse, P. E.; Sittel, K. *J. Appl. Phys.* **1953**, *24*, 690–696.
36. Michaelis, L.; Menten, M. *Biochem. Z.* **1913**, *49*, 333–369.
37. Narita, T.; Knaebel, A.; Munch, J. P.; Candau, S. J. *Macromolecules* **2001**, *34*, 8224–8231.
38. Heyraud, A.; Colin-Morel, P.; Gey, C.; Chavagnat, F.; Guinand, M.; Wallach, J. *Carbohydr. Res.* **1998**, *308*, 417–422.
39. Vandoolaeghe, W. L.; Terentjev, E. M. *J. Phys. A: Math. Gen.* **2007**, *40*, 14725–14744.
40. Catoire, L.; Pierron, M.; Morvan, C.; Herve du Penhoat, C.; Goldberg, R. *J. Biol. Chem.* **1998**, *273*, 33150–33156.
41. Cameron, R. G.; Luzio, G. A.; Goodner, K.; Williams, M. A. K. *Carbohydr. Polym.* **2008**, *71*, 287–299.
42. MacKintosh, F. C.; Käs, J.; Janmey, P. A. *Phys. Rev. Lett.* **1995**, *75*, 4425.
43. Morse, D. C. *Macromolecules* **1998**, *31*, 7044–7067.
44. Zhong, H. J.; Williams, M. A. K.; Goodall, D. M.; Hanson, M. *Carbohydr. Res.* **1998**, *308*, 1–8.
45. Zhong, H. J.; Williams, M. A. K.; Keenan, R. D.; Goodall, D. M. *Carbohydr. Polym.* **1997**, *32*, 27–32.
46. Williams, M. A. K.; Foster, T. J.; Schols, H. A. *J. Agric. Food. Chem.* **2003**, *51*, 1777–1781.
47. Kester, H. C. M.; Visser, J. *Eur. J. Biochem.* **1996**, *240*, 577–585.
48. Ström, A.; Williams, M. A. K. *Carbohydr. Res.* **2004**, *339*, 1711–1716.
49. Goubet, F.; Ström, A.; Dupree, P.; Williams, M. A. K. *Carbohydr. Res.* **2005**, *340*, 1193–1199.
50. Ström, A.; Williams, M. A. K. *J. Phys. Chem.* **2003**, *107*, 10995–10999.
51. Mason, T. G.; Gisler, T.; Kroy, K.; Frey, E.; Weitz, D. A. *J. Rheol.* **2000**, *44*, 917–928.
52. Hemar, H.; Pinder, D. N. *Biomacromolecules* **2006**, *7*, 674–676.
53. Weitz, D. A.; Pine, D. J. In *Dynamic Light Scattering*; Brown, W., Ed.; Oxford University Press: Oxford, 1992.